On Computing the Horizontal Pressure Gradient Force in Sigma Coordinates

MAURICE DANARD, QING ZHANG, AND JOHN KOZLOWSKI

Department of Computer Science, University of Victoria, Victoria, British Columbia, Canada

(Manuscript received 4 January 1993, in final form 1 June 1993)

ABSTRACT

Corby et al. present a finite-difference expression for the horizontal pressure gradient force in sigma coordinates that, in a barotropic atmosphere where the temperature varies linearly with logarithm of pressure, has the same net truncation error as the centered finite-difference approximation for the isobaric geopotential gradient. The requirement that the temperature vary linearly with logarithm of pressure is imposed on analyzed isobaric heights and temperatures using a variational procedure. This reduces the errors in geostrophic winds computed using sigma coordinates. Initial surface pressures and temperatures are calculated in a mesoscale model, assuming the temperature varies linearly with logarithm of pressure and linearly with height. The first method (linear variation with logarithm of pressure) results in smaller errors in computed initial surface geostrophic winds. The structure of a sigma coordinate model is described in which temperature varies linearly with logarithms of pressure. Analytical expressions are derived for the truncation error in the case of temperature varying linearly with height. It is concluded that if a linear variation of temperature with logarithm of pressure is imposed and Corby et al.'s finite difference is employed, then truncation error in the horizontal pressure gradient force will be reduced.

1. Introduction

Sigma coordinates, in which the vertical coordinate is

$$\sigma = \frac{p}{p_s}, \tag{1}$$

where p is pressure and p_s is surface pressure, were introduced by Phillips (1957) and have since been widely adopted. The use of Eq. (1) transforms the earth's surface into the coordinate surface $\sigma = 1$. This is one of the main advantages of using sigma coordinates. Transfers of heat, momentum, and water vapor occur at the earth's surface $\sigma = 1$. The kinematic boundary conditions $\dot{\sigma}(0) = \dot{\sigma}(1) = 0$ are readily applied. However, sigma coordinates are not without problems.

The negative of the horizontal pressure gradient force is, assuming hydrostatic balance,

$$\alpha\nabla_z p = \nabla_p \phi = \nabla_\sigma \phi + RT\nabla \ln p_s, \tag{2}$$

where α is specific volume, ϕ is geopotential, and the subscripts indicate that z, p, or σ is held constant in the horizontal gradient operator.

Consider the last two terms of Eq. (2), that is, the representation in sigma coordinates. These two terms are of opposite sign over sloping terrain. They may each be much larger than their sum. For example, suppose $|\nabla_p \phi| = 10^{-3}$ m s^{-2} at the earth's surface, corresponding to a geostrophic wind of 10 m s^{-1} (for $f = 10^{-4}$ s^{-1}). Suppose that sigma coordinates are employed in a mesoscale model with a terrain slope of 0.1. Then, $|\nabla \phi_s| = 1$ m s^{-2}, where ϕ_s is the geopotential of the earth's surface. Since from Eq. (2) $|\nabla \phi_s + RT\nabla \ln p_s| = 10^{-3}$ m s^{-2}, this means that $RT|\nabla \ln p_s| = 1 \pm 10^{-3}$ m s^{-2}. Obviously, each term must be carefully calculated. Arakawa and Suarez (1983), Corby et al. (1972), Janjic (1977), Kasahara (1974), Kurihara (1968), Mesinger (1982), Mihailovic and Janjic (1986), Nakamura (1978), Simmons and Burrige (1981), Smagorinsky et al. (1967), Sundqvist (1975), and others have discussed this problem.

Mesinger et al. (1988) and Janjic (1990) describe eta or step-mountain models that share the advantages of sigma coordinate models and alleviate the problem with the horizontal pressure gradient force. While the computational benefits of eta coordinates are apparent, the shape of the earth's surface is altered and steps may be introduced where they do not exist in nature. In sigma coordinate models the topography is generally little changed except by smoothing, although problems arise if the slope is steep. In this paper, attention will be confined to sigma coordinate models.

Several investigators (e.g., Sangster 1960, 1987; Phillips 1973; Gary 1973; and Danard 1989) subtract out a reference atmosphere so that each of the last two terms in Eq. (2) is made smaller while their sum is unchanged. However, this will not be done here. In-

Corresponding author address: Dr. Maurice Danard, University of Victoria, Department of Computer Science, P.O. Box 3055, Victoria, British Columbia, Canada V8W 3P6.

stead, it will be shown that use of a simple vertical variation of temperature [Eq. (3)], together with Corby et al.'s (1972) finite-difference scheme [Eqs. (13) and (37)], reduces the error.

In section 2, Corby et al.'s (1972) finite-difference scheme is derived for a barotropic atmosphere with a linear variation of temperature with logarithm of pressure and a nonzero geostrophic wind. The net truncation error is the same as for a centered second-order finite difference of geopotential on an isobaric surface. Section 3 presents a variational method to adjust analyzed isobaric heights and temperatures using the constraint that the temperature varies linearly with the logarithm of pressure between isobaric surfaces. To determine if the adjustments are beneficial, geostrophic winds are computed on sigma surfaces before and after adjustment using Corby et al.'s (1972) finite-difference method and are compared to geostrophic winds calculated from isobaric geopotential gradients. Differences between the two geostrophic winds are reduced by using adjusted data. In sections 4 and 5, initial surface temperatures and pressures are calculated for simple barotropic and baroclinic atmospheres and for an idealized hill assuming two vertical temperature profiles, linear variation with logarithm of pressure, and linear variation with height. The first profile yields more accurate and less noisy surface geostrophic winds calculated using Corby et al.'s (1972) finite-difference procedure. Section 6 gives some concluding remarks, the most important of which is that using Corby et al.'s finite-difference scheme and a linear variation of temperature with logarithm of pressure reduces truncation error in the horizontal pressure gradient force. Appendix A describes a sigma coordinate model in which temperature varies linearly with the logarithm of pressure between sigma surfaces. Temperatures and pressures are initialized in this model from analyzed isobaric data adjusted as described in section 3b. Appendix B gives the truncation error of the horizontal pressure gradient force for the case of temperature varying linearly with height. This profile was used in sections 4 and 5. In appendix C the effect of baroclinity on the finite-difference expression for the horizontal pressure gradient force is examined.

2. Corby's finite-difference scheme

The following derivation of Eq. (13) is similar to that of Corby et al. (1972) except that they assumed a horizontal isobaric surface, which is not the case here. Consider a barotropic atmosphere in which

$$T = A \ln p + B, \tag{3}$$

where A and B are constant. The hydrostatic equation is

$$\frac{\partial \phi}{\partial \ln p} = -RT. \tag{4}$$

Strictly speaking, virtual temperature should be used in Eq. (4) instead of temperature. However, virtual temperature effects will be neglected for simplicity.

Let ϕ_l be the geopotential of the constant sigma surface $\sigma = \sigma_l$ and let $\phi_0(p_0)$ be the geopotential of the isobaric surface $p = p_0$. Substitute Eq. (4) in Eq. (3) and integrate from ϕ_l to ϕ_0:

$$\phi_0 = \phi_l + \frac{RA}{2}[(\ln p_l)^2 - (\ln p_0)^2] + RB(\ln p_l - \ln p_0). \tag{5}$$

Define the difference and averaging operators,

$$\delta_x F = \frac{F(x + \Delta x/2) - F(x - \Delta x/2)}{\Delta x} \tag{6}$$

and

$$\bar{F}^x = \frac{F(x + \Delta x/2) + F(x - \Delta x/2)}{2}, \tag{7}$$

where F is any function. Apply operator (6) to Eq. (5):

$$\delta_x \phi_0 = \delta_x \phi_l + \frac{RA}{2}\delta_x(\ln p_l)^2 + RB\delta_x \ln p_l. \tag{8}$$

Note that p_0 is constant on the isobaric surface $p = p_0$ but p_l is not constant on the sigma surface $\sigma = \sigma_l$. It may be shown that

$$\delta_x F^2 = 2\bar{F}^x \delta_x F. \tag{9}$$

Employing operator (9) in the second term on the right side of Eq. (8) results in

$$\begin{aligned}\delta_x \phi_0 &= \delta_x \phi_l + RA\,\overline{\ln p_l}^x \delta_x \ln p_l + RB\delta_x \ln p_l \\ &= \delta_x \phi_l + R(A\,\overline{\ln p_l}^x + B)\delta_x \ln p_l \\ &= \delta_x \phi_l + R\bar{T}_l^x \delta_x \ln p_l \end{aligned} \tag{10}$$

using Eq. (3). From Eq. (1),

$$\delta_x \ln p_l = \delta_x(\ln \sigma_l + \ln p_s) = \delta_x \ln p_s, \tag{11}$$

since σ_l is constant. Substituting Eq. (11) in Eq. (10) gives

$$\delta_x \phi_0 = \delta_x \phi_l + R\bar{T}_l^x \delta_x \ln p_s. \tag{12}$$

Apply operator (7) to Eq. (12):

$$\delta_x \bar{\phi}_0^x = \delta_x \bar{\phi}_l^x + \overline{R\bar{T}_l^x \delta_x \ln p_s}^x. \tag{13}$$

From Eq. (2) it is seen that Eq. (13) is a centered finite-difference expression for the negative of the x component of the horizontal pressure gradient force. Equation (13) is an identity, provided Eq. (3) holds. Therefore, the right side of Eq. (13) has the same net truncation error as the left side. If ϕ_0 is a linear or quadratic function of x, the net truncation error is zero since the left side of Eq. (13) is then analytically equal to $\partial \phi_0 / \partial x$. If the isobaric surfaces are horizontal, the

left side of Eq. (13) is zero and then two terms on the right side must cancel exactly. Higher-order relationships similar to Eq. (13) that yield zero truncation error for variability greater than quadratic may exist but their derivation is beyond the scope of this paper.

The foregoing results suggest that if Eq. (3) is valid, it is advantageous to calculate the horizontal pressure gradient force in sigma coordinates from the right side of Eq. (13), although it is possible that other finite differences exist with similar properties. Conversely, if the right side of Eq. (13) is used, then it is beneficial to impose Eq. (3). Although only a barotropic atmosphere has been considered so far, it is shown experimentally in the rest of this paper that the foregoing advice is valid in a baroclinic atmosphere as well. The remarks in the rest of this section apply to real as well as to ideal atmospheres.

Assume p_0 is the pressure on the sigma surface at the grid point where Eq. (13) is evaluated. Equation (13) is then a finite-difference form of Eq. (2). Mesinger (1982) points out a problem with Eq. (13) when geopotentials and temperatures are carried at the same sigma surfaces. To illustrate this, note that the left side of Eq. (13) is the difference between two geopotentials, one above and one below the sigma surface (cf. Fig. 1). However, the geopotential at a point depends only on p_s, the surface geopotential ϕ_s, and the temperatures in a vertical column between the earth's surface and the point. Thus, the geopotential in the left side of Eq. (13) that is above the sigma surface depends on temperatures in a portion of the atmosphere that is not used in the right-hand side of Eq. (13).

According to Mesinger (1982) and Janjic (1977), the problem may be alleviated by vertically staggering the temperature and geopotential levels. The geopotential gradients at temperature levels are computed by averaging gradients at geopotential levels above and below the temperature levels. The temperatures and thicknesses between the geopotential levels above and below the temperature levels are hydrostatically consistent. However, the errors on the right side of Eq. (13) will no longer cancel in the ideal case (Mesinger 1982, p. 110). Therefore, in spite of the concerns on Mesinger and Janjic, in the present paper, geopotentials and temperatures will be specified on the same sigma surfaces but in a way that ensures that the vertically integrated hydrostatic equation is satisfied. The problem to which Mesinger and Janjic refer should not be a serious one unless the lapse rate varies significantly in the vertical. This will be alluded to again in section 3c.

3. Adjusting analyzed isobaric temperatures and geopotentials prior to interpolating to sigma surfaces

The thickness between mandatory isobaric surfaces is calculated hydrostatically at radiosondes from temperatures throughout the layer. However, only analyzed temperatures and geopotentials at the top and bottom of the layer are routinely archived. Suppose one has vertical arrays of analyzed isobaric data at horizontally adjacent points and wishes to interpolate to sigma surfaces and use the right side of Eq. (13). It is shown in this section that before doing so it is beneficial to impose Eq. (3) and hydrostatic consistency on the isobaric data.

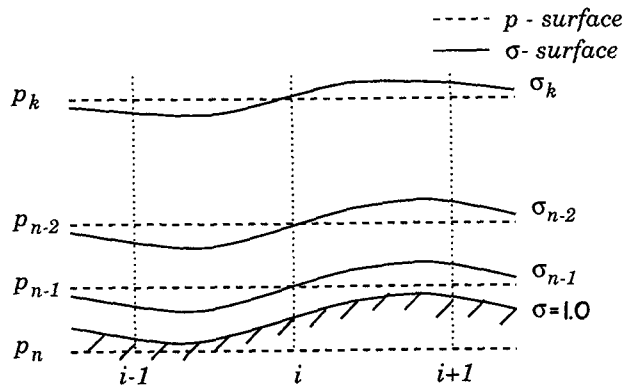

FIG. 1. Vertical spacing of constant pressure and constant sigma surfaces for use in section 3c.

From Eq. (3),

$$T(p) = A_k \ln p + B_k, \quad p_{k-1} \leqslant p \leqslant p_k, \qquad (14)$$

for $k = 2, \cdots, n$. In Eq. (14), A_k and B_k are constants within a given layer at a given point but may vary horizontally and for different layers. Substituting Eq. (14) in Eq. (4) and integrating from p_{k-1} to p_k yields, after some algebra,

$$T_k + T_{k-1} = \frac{2(\phi_{k-1} - \phi_k)}{R \ln(p_k/p_{k-1})}. \qquad (15)$$

Equation (15) may be regarded as an exact finite-difference analog for Eq. (4) (i.e., no truncation error), provided Eq. (14) holds. In general, the isobaric temperatures and geopotentials will not satisfy Eq. (15) at all levels since only temperatures at the top and bottom of each layer are given. The data will be adjusted in a least-squares sense to satisfy Eq. (15) using variational methods.

a. *Adjusting analyzed temperatures only*

Assume first that the analyzed geopotentials are accurate and that only temperatures are to be adjusted. Consider the variational functional

$$I = \sum_{k=1}^{n} \frac{1}{2}(T_{a,k} - T_{o,k})^2 + \sum_{k=2}^{n} \mu_k(T_{a,k} + T_{a,k-1} - f_k), \qquad (16)$$

where the subscripts a and o refer to adjusted and initial temperatures, μ_k is a Lagrange multiplier, and f_k is the right side of Eq. (15). To minimize I, differentiate Eq. (16) partially with respect to $T_{a,m}$ for $m = 1, \cdots, n$ and with respect to μ_m for $m = 2, \cdots, n$. Setting each result to zero yields $(2n - 1)$ linear equations in $(2n - 1)$ unknowns, the n $T_{a,m}$'s, and the $(n - 1)$ μ_m's. This set of equations is solved simultaneously.

Table 1 shows typical results using analyzed Canadian Meteorological Centre data adjusting temperatures only and adjusting both temperatures and geopotentials (to be discussed in section 3b). The data are for a point in the northeastern Pacific Ocean at 0000 UTC 22 December 1979. When only temperatures are adjusted, there is an oscillation in the vertical and temperature changes are unrealistically large. Barker (1980, Figs. 3 and 4) also obtained a sawtooth pattern when calculating temperatures from geopotentials.

A possible explanation for the oscillation is the following. Let

$$\varepsilon_k = T_{a,k} - T_{o,k}, \quad \text{for} \quad k = 1, \cdots, n \tag{17}$$

be the adjustment in temperature and let

$$\eta_k = T_{o,k-1} + T_{o,k} - f_k, \quad \text{for} \quad k = 2, \cdots, n \tag{18}$$

be the amount by which the initial temperatures do not satisfy Eq. (15). The adjusted temperatures satisfy

$$0 = T_{a,k-1} + T_{a,k} - f_k, \quad \text{for} \quad k = 2, \cdots, n. \tag{19}$$

Subtracting Eq. (18) from Eq. (19) gives

$$\varepsilon_{k-1} + \varepsilon_k = -\eta_k. \tag{20}$$

Suppose Eq. (15) is not satisfied in only one layer. That is,

$$\varepsilon_{k-1} + \varepsilon_k = \begin{cases} -\eta_j, & k = j \\ 0, & k \neq j. \end{cases} \tag{21}$$

However, Eq. (21) implies that

$$\varepsilon_{k-1} = -\varepsilon_k, \quad k \neq j. \tag{22}$$

Thus, the temperature adjustments propagate upward and downward from $k = j$, changing sign at each level. The conclusion is that adjusting temperatures only is not a satisfactory procedure.

b. *Adjusting both temperatures and geopotentials*

In this case, one replaces Eq. (16) by

$$I = \sum_{k=1}^{n} \frac{\alpha_k^2}{2}(T_{a,k} - T_{o,k})^2 + \sum_{k=1}^{n} \frac{\beta_k^2}{2}(\phi_{a,k} - \phi_{o,k})^2 + \sum_{k=2}^{n} \mu_k \left[T_{a,k} + T_{o,k-1} - \frac{2(\phi_{a,k-1} - \phi_{a,k})}{R \ln(p_k/p_{k-1})} \right], \tag{23}$$

where α_k^2 and β_k^2 are weights. Barker [1980, Eq. (13)] gives a relation similar to Eq. (23). However, his method of determining weights and use of perturbed idealized data differ from the present paper.

TABLE 1. Typical results for adjusting T only and for adjusting both T and ϕ.

p (mb)	T_0 (°C)	ϕ_0 (m^2 s^{-2})	Adjust T only	Adjust both T and ϕ	
			$(T_a - T_0)$	$(T_a - T_0)$	$(\phi_a - \phi_0)$
100	−55.9	154 683	3.2	0.0	109
150	−55.5	129 429	−4.2	0.0	52
200	−57.3	111 553	3.5	0.0	26
250	−57.4	97 794	−5.6	0.0	−38
300	−53.6	86 554	−0.2	0.0	−192
400	−40.7	67 757	3.4	0.1	−70
500	−29.3	52 450	−1.8	0.2	−31
700	−13.2	28 048	3.2	0.2	17
850	−7.3	13 406	−3.7	0.1	−5
1000	4.5	715	4.2	0.1	1

Equation (23) is minimized by differentiating it partially with respect to $T_{a,m}$ and $\phi_{a,m}$ for $m = 1, \cdots, n$ and with respect to μ_m for $m = 2, \cdots, n$, and setting each result to zero. This yields $(3n - 1)$ linear equations in the $(3n - 1)$ unknowns, the n values of $T_{a,m}$ and $\phi_{a,m}$, and the $(n - 1)$ values of μ_m. As before, the system of equations is solved simultaneously.

To compute the weights, set

$$\alpha_k^2 = \frac{1}{S_{T_k}^2} \tag{24}$$

and

$$\beta_k^2 = \frac{1}{S_{\phi k}^2}, \tag{25}$$

where S_{T_k} and S_{ϕ_k} are the standard errors of T_k and ϕ_k. For simplicity, assume

$$S_{T_k} = S_T = \text{constant}, \tag{26}$$

although it could be argued that S_{T_k} should increase with height as the radiosonde is blown off its launch site. This is because the reported temperature is assumed in the analysis to be located at the radiosonde's surface latitude and longitude. The geopotential is calculated from

$$\phi_k = \phi_s + R \int_{p_k}^{p_s} T d \ln p, \tag{27}$$

where ϕ_s is the surface geopotential. Suppose T has an error δT independent of p (systematic error in the radiosonde). The error in ϕ_k is

$$\delta\phi_k = \delta\phi_s + R\delta T \ln\left(\frac{p_s}{p_k}\right), \tag{28}$$

where $\delta\phi_s$ is the error in ϕ_s. If $\delta\phi_s$ and δT are uncorrelated, Eq. (28) gives

$$S_{\phi_k}^2 = S_{\phi_s}^2 + \left[R \ln\left(\frac{p_s}{p_k}\right)\right]^2 S_T^2. \qquad (29)$$

The last two columns of Table 1 give typical results of adjusting both temperatures and geopotentials with $S_T = 0.5°C$ and $S_{\phi_s} = 10\ m^2\ s^{-2}$. For use in Eq. (29), p_s is assumed to be 1000 mb. Note that the oscillation in $(T_a - T_o)$ is no longer present. The temperatures are changed very little, with most of the adjustment occurring in the geopotentials. This is because the weights β_k^2 defined by Eqs. (25) and (29) decrease with height and become small compared with α_k^2 in Eq. (23). Even if δT varied with height, it is apparent from Eq. (27) that $\delta\phi_k$ depends on the vertically integrated temperature error. The fact that most of the adjustment is forced on ϕ_k would not likely be qualitatively changed.

Sensitivity tests (not shown) were conducted by changing the values of S_T and S_{ϕ_s}. Very little difference was noted. The reason is probably because even at comparatively low heights the second term in Eq. (29) is much larger than the first and for a given isobaric level S_{ϕ_k} is very nearly a constant factor times S_T. Thus, α_k^2 and β_k^2 in Eq. (23) are proportional to each other no matter what the values of S_t and S_{ϕ_s} are. The proportionality factor is a function of p_k only and increases as p_k decreases.

c. *Calculating geostrophic winds from adjusted and unadjusted data*

The purpose of this section is to determine if the adjustment procedure described in section 3b is beneficial. To accomplish this, geostrophic winds are calculated in sigma coordinates from adjusted and unadjusted data and compared to geostrophic winds computed using isobaric geopotentials. The latter winds are assumed to be correct for reasons discussed later in this section.

Sigma levels are set up to coincide with the pressure levels on a point-by-point basis as shown in Fig. 1. At point i, the sigma and isobaric levels coincide. At points $(i + 1)$ and $(i - 1)$, data are interpolated to the sigma surfaces. Geostrophic wind components are calculated in both isobaric and sigma coordinates and compared to each other.

The procedure described in section 3b is applied to isobaric data at the 10 levels given in Table 1 at 0000 UTC 22 December 1979 for the two 5×5 arrays of points shown in Fig. 2. The grid size is 190 km at 60°N.

To calculate surface pressure for elevations less than or equal to the 850-mb height, Eq. (3) is applied to the layer between 850 and 1000 mb:

$$T(p) = A_{10} \ln p + B_{10}, \qquad (30)$$

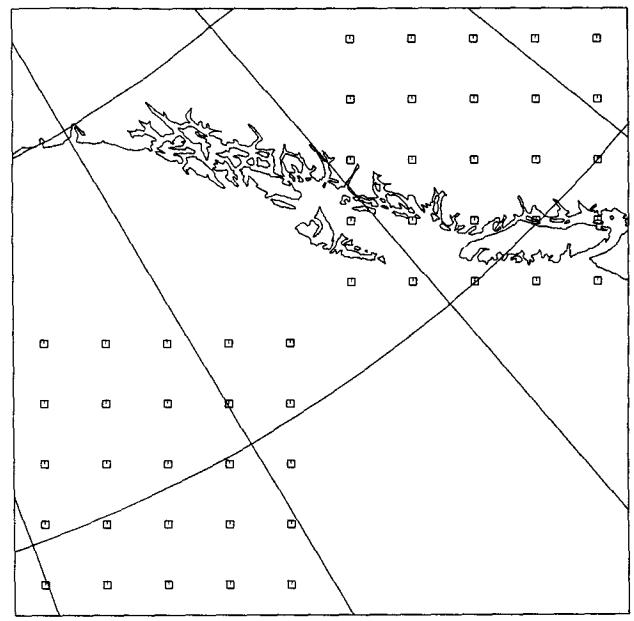

FIG. 2. Arrays of points for which isobaric data are adjusted and geostrophic winds calculated over the northeastern Pacific Ocean and British Columbia.

where

$$A_{10} = \frac{T_{1000} - T_{850}}{\ln(p_{1000}/p_{850})} \qquad (31)$$

and

$$B_{10} = T_{1000} - A_{10} \ln p_{1000}. \qquad (32)$$

Substitute Eq. (30) in Eq. (4) and integrate from p_{1000} to p_s. By analogy to Eq. (5), one obtains

$$\phi_s - \phi_{1000} = -\frac{RA_{10}}{2}[(\ln p_s)^2 - (\ln p_{1000})^2] - RB_{10}(\ln p_s - \ln p_{1000}). \qquad (33)$$

If $A_{10} \neq 0$, Eq. (33) is a quadratic that is solved for $\ln p_s$ using the root with the opposite sign before the radical to the sign of A_{10}. If $A_{10} = 0$, Eq. (33) simplifies to a linear equation in $\ln p_s$. If the 1000-mb height is below the surface, the unadjusted 1000-mb temperature is calculated by downward extrapolation using the standard atmosphere lapse rate. This is not consistent with Eq. (30) but then Eq. (30) does not in general hold for unadjusted data in other layers of the atmosphere. For surface elevations above 850 mb, a similar procedure is used except that data for the layer 700–850 mb are used.

Once surface pressures are calculated (for point i in Fig. 1), set

$$\sigma_k = \frac{p_k}{p_{s,i}}, \quad \text{if} \quad p_k \leq p_{s,i} \text{ for } k = 1, \cdots, (n-1).$$

TABLE 2. Root-mean-square errors of u_g over the ocean computed from Eq. (37a) using adjusted and unadjusted data.

p (mb)	Mean u_g (m s^{-1})	rms errors (m s^{-1})	
		Adjusted	Unadjusted
100	28	0.66	0.93
150	33	0.71	1.18
200	35	0.61	0.62
250	39	1.50	1.83
300	40	2.36	2.46
400	37	1.72	1.83
500	32	0.74	1.31
700	26	1.15	1.80
850	22	0.50	0.92
1000	18	0.10	0.02
Average	31	1.20	1.46

TABLE 3. Root-mean-square errors of v_g over the ocean computed from Eq. (37b) using adjusted and unadjusted data.

p (mb)	Mean v_g (m s^{-1})	rms errors (m s^{-1})	
		Adjusted	Unadjusted
100	19	1.83	2.72
150	19	1.37	2.28
200	19	1.16	1.78
250	18	0.67	1.56
300	18	0.80	0.68
400	16	0.77	1.06
500	14	1.10	1.47
700	12	1.64	2.20
800	12	0.26	0.49
1000	11	0.07	0.01
Average	16	1.11	1.66

For points $i \pm 1$, the pressures on the sigma surface are

$$p_{i\pm1}(\sigma_k) = \sigma_k p_{s,i\pm1}.$$

To compute $T_{i-1}(\sigma_k)$ and $\phi_{i-1}(\sigma_k)$, assume for illustrative purposes that $p_{i-1}(\sigma_k) > p_k$. From Eq. (3) one obtains

$$T_{i-1}(\sigma_k) = T_{i-1}(p_k) + \frac{[T_{i-1}(p_{k+1}) - T_{i-1}(p_k)]}{\ln(p_{k+1}/p_k)} \ln\left[\frac{p_{i-1}(\sigma_k)}{p_k}\right]. \quad (34)$$

By analogy to Eq. (15),

$$\phi_{i-1}(\sigma_k) = \phi_{i-1}(p_k) + \frac{R}{2}[T_{i-1}(\sigma_k) + T_{i-1}(p_k)] \ln\left[\frac{p_{i-1}(\sigma_k)}{p_k}\right]. \quad (35)$$

If $p_{i-1}(\sigma_k) < p_k$, simply replace p_{k+1} in Eq. (34) and Eq. (35) by p_{k-1}. Values for point $(i + 1)$ are calculated in a similar manner. Note that points $i \pm 1$ are on different sides of the isobaric surface $p = p_k$ (i.e., one is above and the other is below). Therefore, they do not have the same A_k in Eq. (14). This is a source of some error in the results described in the following. It is an example of the problem with Corby et al.'s (1972) scheme that Mesinger (1982) refers to and which is discussed at the end of section 2.

The geostrophic wind components in isobaric coordinates are calculated from [cf. Eq. (13)]

$$u_{gk} = -f^{-1}\delta_y \bar{\phi}^y(p_k) \quad (36a)$$

and

$$v_{gk} = f^{-1}\delta_x \bar{\phi}^x(p_k). \quad (36b)$$

In σ coordinates, the corresponding expressions are

$$u_{gk} = -f^{-1}[\delta_y \bar{\phi}^y(\sigma_k) + \overline{R\bar{T}^y(\sigma_k)\delta_y \ln p_s}^y] \quad (37a)$$

and

$$v_{gk} = f^{-1}[\delta_x \bar{\phi}^x(\sigma_k) + \overline{R\bar{T}^x(\sigma_k)\delta_x \ln p_s}^x]. \quad (37b)$$

Equations (36) and (37) are evaluated over the water and land arrays of points shown in Fig. 2. The correct geostrophic components are assumed to be given by Eqs. (36) applied to the unadjusted isobaric heights. The reason for assuming that geostrophic winds computed from unadjusted isobaric geopotentials are correct is to avoid introducing a bias in favor of geostrophic winds calculated in sigma coordinates from adjusted data. In fact, if there is any bias, it favors geostrophic winds computed in sigma coordinates from unadjusted data. Tables 2–5 show the root-mean-square errors of using Eqs. (37a) and (37b) with adjusted and unadjusted data.

Tables 2 and 3 clearly show it is generally better to use adjusted data, except at 1000 mb where errors are negligible. Tables 4 and 5 give similar results for land points. The differences between using adjusted and unadjusted data resemble those in Tables 2 and 3. This is surprising, since one might expect greater improvement over sloping (land) surfaces than over horizontal

TABLE 4. Root-mean-square errors of u_g over mountainous terrain computed from Eq. (37a) using adjusted and unadjusted data.

p (mb)	Mean u_g (m s^{-1})	rms errors (m s^{-1})	
		Adjusted	Unadjusted
100	8	1.95	2.58
150	6	1.56	2.25
200	5	1.43	1.47
250	3	1.31	1.89
300	0	0.88	0.91
400	−4	1.39	1.62
500	−2	1.81	2.03
700	6	0.48	0.56
850	10	0.65	0.78
Average	4	1.27	1.57

TABLE 5. Root-mean-square errors of v_g over mountainous terrain computed from Eq. (37b) using adjusted and unadjusted data.

p (mb)	Mean v_g (m s^{-1})	rms errors (m s^{-1})	
		Adjusted	Unadjusted
100	30	1.37	1.89
150	25	1.29	1.47
200	24	1.71	2.21
250	22	0.67	0.88
300	23	1.00	1.32
400	23	0.97	1.36
500	19	0.66	0.86
700	10	0.70	0.92
850	7	0.20	0.37
Average	20	0.95	1.25

(ocean) surfaces. Perhaps baroclinic effects, to be discussed later in section 5 and appendix C, are important.

Table 6 shows the overall reduction in rms errors (last lines of Tables 2–5) when adjusted data are used instead of unadjusted data. Also given are the significance levels of the differences in the error variances. These are obtained by applying the F test to the ratio of the two variances (unadjusted divided by adjusted). The most significant difference is for v_g over the ocean.

The use of isobaric heights and temperatures, adjusted as described in section 3b, to initialize a sigma coordinate model is described in appendix A. This model also imposes the requirement that temperatures vary linearly with pressure between the sigma surfaces during the time integration, and it makes use of the right side of Eq. (13).

4. Computing initial surface pressure and temperature in a mesoscale model

The purpose of sections 4 and 5 is to compare the results of initializing surface pressure and temperature using two vertical profiles—one linear in logarithm of pressure [Eq. (3)] and the other linear in height [Eq. (44)]—in a model where the horizontal pressure gradient force is calculated using Eq. (13). To facilitate this collation, initial surface geostrophic winds are calculated for the two profiles using Eq. (37) and are compared to analytical values. Idealized atmospheres and idealized terrain are employed.

Suppose one is given the initial 850-mb height and temperature (Z_{850}, T_{850}) everywhere and the surface height and initial temperature (Z_{sr}, T_{sr}) (but not pressure) at a reference point. The surface temperature is at the screen or anemometer level where winds are nonzero. Two methods of calculating the initial surface pressure and temperature ($\ln p_s$, T_s) at any point will be employed and the computed pressure gradients compared.

One method makes use of Eq. (3) where A is constant and B may be a function of x and y. The reference

TABLE 6. Overall percent improvement in rms errors using adjusted rather than unadjusted data, and significance level of ratio of square of rms errors. See last lines of Tables 2–5.

Surface	Component	Percent improvement	Significance level (%)
Ocean	u_g	18	20
	v_g	33	2.5
Land	u_g	19	20
	v_g	24	10

point surface pressure may be obtained from Eq. (15) assuming the kth level is at the surface and the $(k-1)$th level is at 850 mb. This gives

$$\ln p_{sr} = \frac{2g(Z_{850r} - Z_{sr})}{R(T_{850r} + T_{sr})} + \ln p_{850}. \tag{38}$$

Employing Eq. (3) at the reference point both at the surface and 850 mb and subtracting yields

$$A = \frac{T_{sr} - T_{850r}}{\ln(p_{sr}/p_{850})}. \tag{39}$$

The atmospheres in sections 4 and 5 are ideal ones in which Eqs. (3) and (39) hold by definition. In real atmospheres with strong surface heating or cooling, Eq. (3) may not be appropriate next to the earth's surface. Since A is assumed constant, Eq. (39) may be written for any point so that

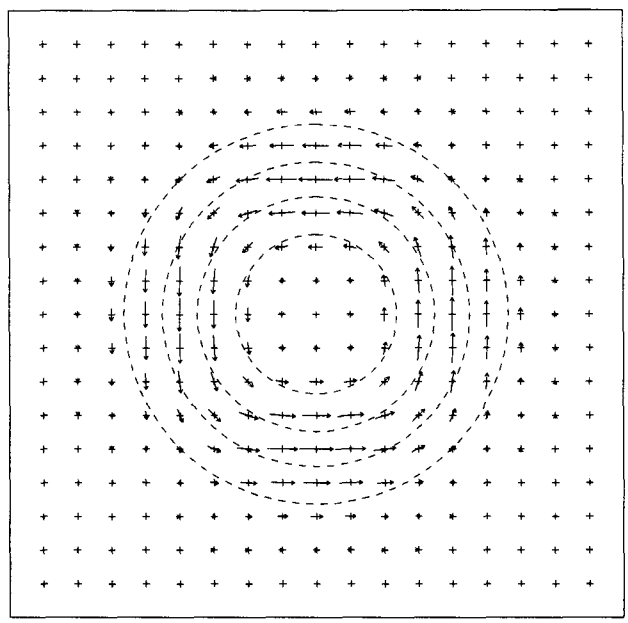

FIG. 3. Vector error (computed minus analytical) in surface geostrophic winds calculated from Eqs. (37a) and (37b) using Eq. (44) for a hill height of 5000 m, a barotropic atmosphere, and horizontal isobaric surfaces. A vector length of one grid distance represents 0.62 m s^{-1}. Dashed lines are the 1000-, 2000-, 3000-, and 4000-m height contours.

TABLE 7. Maximum magnitude (m s^{-1}) of vector error in computed surface geostrophic wind for barotropic atmosphere with horizontal isobaric surfaces.

Temperature variation	Hill height (km)				
	1	2	3	4	5
$T = A \ln p + B$	3.0×10^{-12}	2.7×10^{-12}	3.1×10^{-12}	4.7×10^{-12}	7.9×10^{-12}
$T = A'z + B'$	0.004	0.036	0.125	0.302	0.603

$$\frac{T_s - T_{850}}{\ln(p_s/p_{850})} = \frac{T_{sr} - T_{850r}}{\ln(p_{sr}/p_{850})}. \quad (40)$$

Similarly, Eq. (38) gives for any point

$$\ln p_s = \frac{2g(Z_{850} - Z_s)}{R(T_{850} + T_s)} + \ln p_{850}. \quad (41)$$

Equations (40) and (41) contain two unknowns, $\ln p_s$ and T_s. Solving each equation for $\ln(p_s/p_{850})$ and equating yields

$$T_s = \left[T_{850}^2 + \frac{2g(Z_{850} - Z_s)(T_{sr} - T_{850})}{R \ln(p_{sr}/p_{850})} \right]^{1/2}. \quad (42)$$

Substituting for $\ln(p_{sr}/p_{850})$ from Eq. (38) results in

$$T_s = \left[T_{850}^2 + \frac{(Z_{850} - Z_s)(T_{sr} - T_{850r})}{(Z_{850r} - Z_{sr})(T_{sr} + T_{850r})} \right]^{1/2}. \quad (43)$$

Once T_s is evaluated, it is substituted in Eq. (41) to give $\ln p_s$.

The second method to calculate initial surface pressure and temperature is to replace Eq. (3) with

$$T = A'z + B', \quad (44)$$

where A' is a constant and B' may be a function of x and y. The coefficient A' is computed from

$$A' = \frac{T_{850r} - T_{sr}}{Z_{850r} - Z_{sr}} \quad (45)$$

and T_s from

$$T_s = T_{850} - A'(Z_{850} - Z_s). \quad (46)$$

To find the initial surface pressure, integrate Eq. (4) from 850 mb to the surface to give

$$\ln p_s = \ln p_{850} + \frac{g}{R} \int_{Z_s}^{Z_{850}} \frac{dz}{T}. \quad (47)$$

If $A' \neq 0$, from Eq. (44) one has $dz = dT/A'$, so Eq. (47) becomes

$$\ln p_s = \ln p_{850} + \frac{g}{RA'} \ln\left(\frac{T_{850}}{T_s}\right). \quad (48)$$

If $A' = 0$, then $T = T_{850}$ in Eq. (47), and so

$$\ln p_s = \ln p_{850} + \frac{g(Z_{850} - Z_s)}{RT_{850}}. \quad (49)$$

Equation (44) has been used in boundary-layer modeling (e.g., Danard 1977; Mass and Dempsey 1985; Achtemeier 1991). Carroll et al. (1987) assume a linear variation of potential temperature with height. However, it is shown in section 5 that if Eqs. (37) are employed to calculate initial surface geostrophic winds, Eq. (3) results in less noise than does Eq. (44). The truncation error resulting from using Eqs. (44) and (37) is derived in appendix B.

5. Comparing calculated initial surface geostrophic winds

Consider the idealized hill whose surface elevation is given by

$$Z_s = \begin{cases} \dfrac{h}{2}\left[1 + \cos\left(\dfrac{2\pi s}{L}\right)\right], & s \leq \dfrac{L}{2} \\ 0, & s > \dfrac{L}{2} \end{cases}, \quad (50)$$

where h is the height of the hill, $s = (x^2 + y^2)^{1/2}$ is the horizontal distance from the apex to a point, and L is the hill width.

The computations described in section 4 are applied to a hill of width $L = 80$ km with a horizontal grid size of 5 km. Five different hill heights ($h = 1$, 2, 3, 4, and 5 km) are employed. Calculations are performed for

TABLE 8. Maximum magnitude (m s^{-1}) of vector error in computed surface geostrophic wind or barotropic atmosphere with 850-mb geostrophic wind of 10 m s^{-1} at 026°.

Temperature variation	Hill height (km)				
	1	2	3	4	5
$T = A \ln p + B$	4.5×10^{-12}	4.1×10^{-12}	4.8×10^{-12}	4.6×10^{-12}	4.9×10^{-12}
$T = A'z + B'$	0.004	0.033	0.113	0.279	0.546

four atmospheres: barotropic with horizontal isobaric surface, barotropic with constant 850-mb geostrophic wind, baroclinic with constant 850-mb geostrophic wind, and two values of the isobaric temperature gradient. In all experiments $A = 49.8°C$ and $A' = 5.84 \times 10^{-3}°C\ m^{-1}$. In each case the initial surface geostrophic wind can be analytically computed and compared to values calculated from Eqs. (37a) and (37b) using Eqs. (3) and (44).

Figure 3 gives the vector error (computed minus analytical) using Eq. (44) for a hill height of 5 km with a barotropic atmosphere and horizontal isobaric surfaces. In this case the initial analytic geostrophic wind is zero. Note that the largest errors occur halfway up the hill where the terrain slope is steepest. The use of Eq. (44) results in a spurious cyclonic geostrophic wind. The errors using Eq. (3) (not plotted) are 11 orders of magnitude smaller and would simply show as dots if plotted using the same scale as Fig. 3. This is to be expected from Eq. (13).

Tables 7–10 give maximum errors for the five hill heights, four atmospheres, and two vertical temperature variations. In Table 7, when Eq. (3) is used, errors are essentially zero at all heights. However, when Eq. (44) is employed, errors are significant and increase with hill height. In Table 8, errors using Eq. (3) are still negligible. The errors in Table 8 using Eq. (44) are, surprisingly, smaller than in Table 7 for $h = 2$, 3, 4, and 5 km. In Tables 9 and 10 (baroclinic atmospheres), Eq. (3) gives smaller errors than Eq. (44), with the difference between the two errors increasing with increasing hill height. However, the differences are not so marked as in the barotropic cases (Tables 7 and 8). A possible explanation for the relatively small improvement in the baroclinic cases is given in appendix C.

6. Summary and conclusions

By slightly modifying Corby et al.'s (1972) derivation, it is shown in section 2 that if the temperature varies linearly with logarithm of pressure in a barotropic atmosphere and the isobaric height is a linear or quadratic function of x, then calculating the horizontal pressure gradient force in sigma coordinates from the finite-difference expression (13) results in zero net truncation error.

TABLE 9. Maximum magnitude ($m\ s^{-1}$) of vector error in computed surface geostrophic wind for baroclinic atmosphere with $(\partial T/\partial x)_p = 1.0 \times 10^{-5}°C\ m^{-1}$ and 850-mb geostrophic wind of 10 $m\ s^{-1}$ at 026°.

Temperature variation	Hill height (km)				
	1	2	3	4	5
$T = A \ln p + B$	0.058	0.110	0.163	0.218	0.272
$T = A'z + B'$	0.059	0.115	0.180	0.314	0.558

TABLE 10. Maximum magnitude ($m\ s^{-1}$) of vector error in computed surface geostrophic wind for baroclinic atmosphere with $(\partial T/\partial x)_p = 2.0 \times 10^{-5}°C\ m^{-1}$ and 850-mb geostrophic wind of 10 $m\ s^{-1}$ at 026°.

Temperature variation	Hill height (km)				
	1	2	3	4	5
$T = A \ln p + B$	0.118	0.221	0.333	0.459	0.651
$T = A'z + B'$	0.119	0.230	0.352	0.481	0.724

In section 3, the logarithmic variation of temperature is imposed on analyzed isobaric heights and temperatures using a variational procedure. To determine if the resulting adjustments are beneficial, geostrophic winds are calculated in isobaric and sigma coordinates from unadjusted and adjusted data. When the logarithmic constraint is imposed, errors using sigma coordinates and Eq. (37), which is based on Eq. (13), are smaller than when the constraint is not imposed.

In section 4, methods are described to calculate initial surface pressure and temperature in a mesoscale model assuming the temperature varies linearly with logarithm of pressure and linearly with height. In section 5, initial surface geostrophic winds are computed in sigma coordinates using both temperature profiles and compared to analytically calculated geostrophic winds. The linear variation with logarithm of pressure gives smaller errors than the linear variation with height. The truncation error for the case of linear variation with height is derived in appendix B for a barotropic atmosphere with a constant lapse rate. Only if the atmosphere is isothermal or the earth's surface is an isobaric surface will linear variation with height result in the same net truncation error as linear variation with logarithm of pressure.

At the end of section 2 and in section 3c, reference is made to possible difficulties associated with calculating geopotentials and temperatures at the same levels. However, these problems appear not to be serious ones.

The findings in this paper support the conclusion that imposing a linear variation of temperature with logarithm of pressure [Eq. (3)] and calculating the horizontal pressure gradient force using the right side of Eq. (13) will significantly reduce truncation error in atmospheric models using sigma coordinates. However, it is not intended to imply that Eqs. (3) and (13) are necessarily the only pair of relationships producing this desirable result. Subtracting out a reference atmosphere (see section 1) should help further in reducing truncation error.

Acknowledgments. This research has been supported by the Natural Sciences and Engineering Research Council of Canada.

APPENDIX A

Application to a Sigma Coordinate Model

The structure of a model that employs sigma coordinates assumes a linear variation of temperature with logarithm of pressure, and uses the right side of Eq. (13) will be described. Temperatures and geopotentials are computed at the same sigma surfaces, notwithstanding the concerns of Mesinger (1982) discussed at the end of section 2.

Suppose one has initial isobaric heights and temperatures at all levels of the atmosphere that have been adjusted as described in section 3b. The initial surface pressure and temperature (i.e., at $\sigma = 1$) are computed from Eqs. (30)–(33). Equations (31) and (32) are first evaluated, and Eq. (33) is then solved for $\ln p_s$. The surface temperature is found from Eq. (30) with $\ln p$ replaced by $\ln p_s$. For the sigma levels above the earth's surface, suppose $\sigma = \sigma_l$ lies between the isobaric surfaces $p = p_k$ and $p = p_{k+1}$ ($>p_k$). See Fig. A1. The temperature and height at $\sigma = \sigma_l$ are found from equations similar to Eqs. (34) and (35):

$$T(\sigma_l) = T(p_k) + \frac{[T(p_{k+1}) - T(p_k)]}{\ln(p_{k+1}/p_k)} \ln\left[\frac{p(\sigma_l)}{p_k}\right], \tag{A1}$$

and

$$\phi(\sigma_l) = \phi(p_k) + \frac{R}{2}[T(\sigma_l) + T(p_k)] \ln\left[\frac{p(\sigma_l)}{p_k}\right]. \tag{A2}$$

Starting from initial values of T and ϕ at all N sigma levels ($\sigma_1, \sigma_2, \cdots, \sigma_N = 1$) computed as described above, one computes new temperatures from the thermodynamic equation and new geopotentials from the hydrostatic equation

$$\phi_l = \phi_{l+1} + R \ln\left(\frac{\sigma_{l+1}}{\sigma_l}\right)\left(\frac{T_l + T_{l+1}}{2}\right), \quad l = (N-1), (N-2), \cdots, 1, \tag{A3}$$

where $\phi_N = \phi_s$. Note the similarity of Eqs. (15) and (A3). No adjustment of heights and temperatures is carried out during the time integration. However, the requirement that the temperature vary linearly with logarithm of pressure between the sigma surfaces implicit in Eq. (A3) ensures that the truncation error is small.

APPENDIX B

Truncation Error for $T = A'z + B'$

A barotropic atmosphere will be assumed (temperatures constant on isobaric surfaces). Consider first the case where $A' = 0$. From Eq. (49),

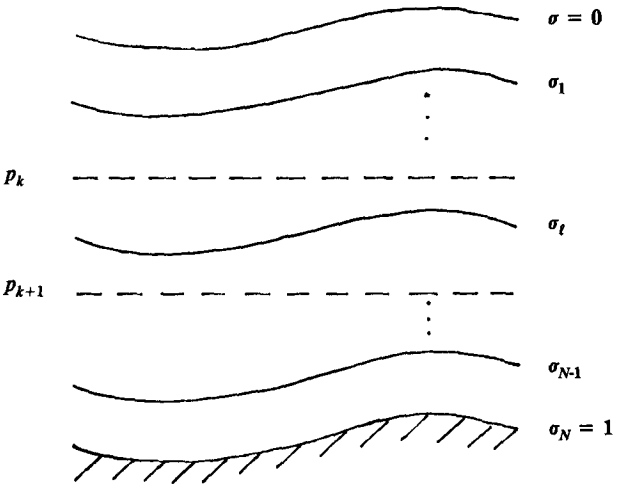

FIG. A1. Structure of a sigma coordinate model. Solid lines are constant sigma surfaces; dashed lines are isobaric surfaces.

$$\delta_x \ln p_s = \frac{g}{RT_{850}} \delta_x(Z_{850} - Z_s). \tag{B1}$$

However, since the atmosphere is isothermal, $T_{850} = \bar{T}_s^x$, so Eq. (A4) may be written

$$g\delta_x Z_{850} = g\delta_x Z_s + R\bar{T}_s^x \delta_x \ln p_s. \tag{B2}$$

Comparing Eqs. (B2) and (12), it is seen that for isothermal conditions, Eq. (44) is just as good as Eq. (3). This is not surprising, since $A' = 0$ is simply a special case of Eq. (3) with $A = 0$.

For the case $A' \neq 0$, note from Eq. (48) that

$$\delta_x \ln p_s = -\frac{g}{RA'} \delta_x \ln T_s. \tag{B3}$$

From Eq. (6),

$$\delta_x \ln T_s = \frac{\ln T_s(x + \Delta x/2) - \ln[T_s(x - \Delta x/2)]}{\Delta x} = \frac{1}{\Delta x} \ln\left[\frac{T_s(x + \Delta x/2)}{T_s(x - \Delta x/2)}\right] = \frac{1}{\Delta x} \ln\left[1 + \frac{\Delta x \delta_x T_s}{T_s(x - \Delta x/2)}\right].$$

Expanding the logarithm gives

$$\delta_x \ln T_s = \frac{\delta_x T_s}{T_s(x - \Delta x/2)} - \frac{1}{2}\left[\frac{\delta_x T_s}{T_s(x - \Delta x/2)}\right]^2 \Delta x + O[(\delta_x T_s)^3 (\Delta x)^2]. \tag{B4}$$

From Eq. (46),

$$\delta_x T_s = -A'\delta_x Z_{850} + A'\delta_x Z_s. \tag{B5}$$

Substitute Eq. (B5) in the first term on the right side of Eq. (B4) and then substitute Eq. (B4) in Eq. (B3). This results in

$$g\delta_x Z_{850} = g\delta_x Z_s + RT_s(x - \Delta x/2)\delta_x \ln p_s - \frac{g}{2A'}\frac{(\delta_x T_s)^2 \Delta x}{T_s(x - \Delta x/2)} + O[(\delta_x T_s)^3(\Delta x)^2]. \quad \text{(B6)}$$

Comparing Eqs. (B6) and (12), it is seen that only if T_s is constant will these two expressions be equal. Since T_{850} and A' are constant, this will occur only if the earth's surface is an isobaric surface. Only in this case will Eq. (44) result in the same net truncation error as Eq. (3). Note that the largest difference between Eqs. (B6) and (12) occurs where T_s varies rapidly. In Fig. 3, this is halfway up the hill where the terrain slope is greatest. The limit of Eq. (B6) as $\Delta x \to 0$ gives Eq. (12).

APPENDIX C

Horizontal Pressure Gradient Force for a Simple Baroclinic Atmosphere

Consider the simple baroclinic case where B varies with x and y but not with p. Equation (5) is unchanged but Eq. (8) is replaced by

$$\delta_x \phi_0 = \delta_x \phi_l + \frac{RA}{2}\delta_x(\ln p_l)^2 + R\delta_x[B(\ln p_l - \ln p_0)]. \quad \text{(C1)}$$

To expand the last two terms of Eq. (C1), one makes use of Eq. (9) and a similar identity

$$\delta_x(FG) = \bar{F}^x \delta_x G + \bar{G}^x \delta_x F. \quad \text{(C2)}$$

Then Eq. (C1) becomes

$$\begin{aligned}\delta_x \phi_0 &= \delta_x \phi_l + RA\,\overline{\ln p_l}^x \delta_x \ln p_l + R\bar{B}^x \delta_x \ln p_l \\ &\quad + R(\overline{\ln p_l}^x - \ln p_0)\delta_x B \\ &= \delta_x \phi_l + R\overline{(A \ln p_l + B)}^x \delta_x \ln p_l \\ &\quad + R(\overline{\ln p_l}^x - \ln p_0)\delta_x B \\ &= \delta_x \phi_l + R\bar{T}_l^x \delta_x \ln p_s \\ &\quad + R(\overline{\ln p_l}^x - \ln p_0)\delta_x B, \quad \text{(C3)}\end{aligned}$$

where Eq. (11) has been used in the second term on the right side of Eq. (C3).

Comparing Eqs. (C3) and (12), one sees that the last term in Eq. (C3) represents the effect of baroclinity. If $p_0 \neq p_l$, one would expect this term to be nonzero from the thermal wind equation. However, even if $p_0 = p_l$, the baroclinic term does not vanish unless $\overline{\ln p_l}^x = \ln p_0$. This may explain why the advantages of using Eq. (3) rather than Eq. (44) are less pronounced in baroclinic than in barotropic atmospheres. (See last paragraph of section 5.)

REFERENCES

Achtemeier, G. L., 1991: Reducing hydrostatic truncation error in a mesobeta boundary layer model. *Mon. Wea. Rev.*, **119,** 223–229.

Arakawa, A., and M. J. Suarez, 1983: Vertical differencing of the primitive equations in sigma coordinates. *Mon. Wea. Rev.*, **111,** 34–56.

Barker, E. H., 1980: Solving for temperature using unnaturally latticed hydrostatic equations. *Mon. Wea. Rev.*, **108,** 1260–1268.

Carroll, J. J., L. R. Mendez-Nunez, and S. Tanrikulu, 1987: Accurate pressure gradient calculations in hydrostatic atmospheric models. *Bound.-Layer Meteor.*, **41,** 149–169.

Corby, G. A., A. Gilchrist, and R. L. Newson, 1972: A general circulation model of the atmosphere suitable for long period integrations. *Quart. J. Roy. Meteor. Soc.*, **98,** 809–832.

Danard, M. B., 1977: A simple model for mesoscale effects of topography on surface winds. *Mon. Wea. Rev.*, **105,** 572–581.

——, 1989: On computing the surface horizontal pressure gradient over elevated terrain. *Mon. Wea. Rev.*, **117,** 1344–1350.

Gary, J. M., 1973: Estimate of truncation error in transformed coordinate, primitive equation atmospheric models. *J. Atmos. Sci.*, **30,** 223–233.

Janjic, Z. I., 1977: Pressure gradient force and advection scheme used for forecasting with steep and small scale topography. *Contrib. Atmos. Phys.*, **50,** 186–199.

——, 1990: The step-mountain coordinate: Physical package. *Mon. Wea. Rev.*, **118,** 1429–1443.

Kasahara, A., 1977: Computational aspects of atmospheric simulation. *Methods Comput. Phys.*, **17,** 1–55.

Kurihara, Y., 1968: Note on the finite difference expressions for the hydrostatic relation and pressure gradient force. *Mon. Wea. Rev.*, **96,** 654–656.

Mass, C. F., and D. P. Dempsey, 1985: A one-level mesoscale model for diagnosing surface winds in mountainous and coastal regions. *Mon. Wea. Rev.*, **113,** 1211–1227.

Mesinger, F., 1982: On the convergence and error problems of the calculation of the pressure gradient force in sigma coordinate models. *Geophys. Astrophys. Fluid Dyn.*, **19,** 105–117.

——, Z. Janjic, S. Nickovic, D. Gavrilov, and D. Deaven, 1988: The step-mountain coordinate: Model description and performance for cases of alpha lee cyclogenesis and for a case of Appalachian redevelopment. *Mon. Wea. Rev.*, **116,** 1493–1518.

Mihailovic, D. T., and Z. I. Janjic, 1986: Comparison of methods for reducing the error of the pressure gradient force in sigma coordinate models. *Meteor. Atmos. Phys.*, **35,** 177–184.

Nakamura, H., 1978: Dynamical effects of mountains on the general circulation of the atmosphere. I: Development of finite difference schemes suitable for incorporating mountains. *J. Meteor. Soc. Japan*, **56,** 317–339.

Phillips, N. A., 1957: A coordinate system having some special advantages for numerical forecasting. *J. Meteor.*, **14,** 184–185.

——, 1973: Principles of large scale numerical weather prediction. *Dynamic Meteorology*, P. Morel, Ed., D. Reidel Pub. Co., 1–96.

Sangster, W. E., 1960: A method of representing the horizontal pressure gradient force without reduction of station pressure to sea level. *J. Meteor.*, **17,** 166–176.

——, 1987: An improved technique for computing the horizontal pressure gradient force at the earth's surface. *Mon. Wea. Rev.*, **115,** 1358–1369.

Simmons, A. J., and D. M. Burridge, 1981: An energy and angular-momentum conserving vertical finite-difference scheme and hybrid vertical coordinates. *Mon. Wea. Rev.*, **109,** 758–770.

Smagorinsky, J., R. F. Strickler, W. E. Sangster, S. Manabe, J. L. Holloway, and G. D. Hembree, 1967: Prediction experiments with a general circulation model. *Proc. Symp. on Dynamics of Large Scale Atmospheric Processes*, Moscow, 70–134.

Sundqvist, H., 1975: On truncation errors in sigma-system models. *Atmosphere*, **13,** 81–95.